

Expression of Novel Molecules, MICAL2-PV (MICAL2 Prostate Cancer Variants), Increases with High Gleason Score and Prostate Cancer Progression

Shingo Ashida,^{1,2} Mutsuo Furihata,³ Toyomasa Katagiri,¹ Kenji Tamura,^{1,2} Yoshio Anazawa,¹ Hiroki Yoshioka,¹ Tsuneharu Miki,⁴ Tomoaki Fujioka,⁵ Taro Shuin,² Yusuke Nakamura,¹ and Hidewaki Nakagawa¹

Abstract Purpose: The aim of this study is to identify novel molecular targets for development of novel treatment or diagnostic markers of prostate cancer through genome-wide cDNA microarray analysis of prostate cancer cells purified by laser microdissection.

Experimental Design and Results: Here, we identified *molecule interacting with CasL-2 prostate cancer variants (MICAL2-PV)*, novel splicing variants of *MICAL2*, showing overexpression in prostate cancer cells. Immunohistochemical analysis using an antibody generated specific to MICAL2-PV revealed that MICAL2-PV was expressed in the cytoplasm of cancer cells with various staining patterns and intensities, whereas it was not or hardly detectable in adjacent normal prostate epithelium or prostatic intraepithelial neoplasia. Interestingly, immunohistochemical analysis of 105 prostate cancer specimens on the tissue microarray indicated that MICAL2-PV expression status was strongly correlated with Gleason scores ($P < 0.0001$) or tumor classification ($P < 0.0001$). Furthermore, the expression levels of MICAL2-PVs were also concordant to those of c-Met, a marker of tumor progression, with statistical significance ($P = 0.0018$). To investigate its potential of molecular therapeutic target for prostate cancers, we knocked down endogenous *MICAL2-PVs* in prostate cancer cells by small interfering RNA, which resulted in the significant reduction of prostate cancer cell viability.

Conclusions: Our findings suggest that MICAL2-PV is likely to be involved in cancer progression of prostate cancer and could be a candidate as a novel molecular marker and/or target for treatment of prostate cancers with high Gleason score.

Prostate cancer is the most common malignancy in males and the second leading cause of cancer-related deaths in the United States and Europe (1). Detection of prostate cancer at an early stage by serum test for prostate-specific antigen (PSA) and subsequent surgery, and radiation therapy can cure the localized disease, but nearly 30% of treated prostate cancer patients suffer relapse (2–4). Relapsed or advanced prostate cancers are usually treated with androgen ablation therapy and reveal relatively good response, but some of them eventually become androgen independent and progress very rapidly.

Because there is at present no effective therapy available for such advanced tumors, it is crucial to develop novel therapeutic tools against prostate cancers.

To attempt to identify novel molecular targets or biological markers for prostate cancers, we previously analyzed the precise gene expression profiles of prostate cancer cells purified by laser microdissection by using a genome-wide cDNA microarray (5). In the present study, we report the identification and characterization of *molecule interacting with CasL-2 prostate cancer variants (MICAL2-PV)*, which are novel splicing variants of *MICAL2* belonging to the *MICAL* family, overexpressed in prostate cancer cells. *MICAL1* was initially identified as a CasL-interacting molecule and was shown to associate with vimentin, a cytoskeletal regulator that connects CasL to intermediate filaments (6). In addition, Terman et al. have reported that *Drosophila* *MICAL1* interacts with the neuronal plexin A receptor and is required for semaphorin 1a/plexin A-mediated repulsive axon guidance during neural development (7). It is also known that semaphorins and plexins are involved in control of invasive growth of cancer cells through making a complex with and activating c-Met (hepatocyte growth factor receptor; refs. 8–10). Although *MICAL2* and its novel variants *MICAL2-PVs* have a high degree of homology and share several important domains with *MICAL1*, little is known about their pathophysiologic roles in growth of tumor cells or in neuronal guidance and development.

Authors' Affiliations: ¹Laboratory of Molecular Medicine, Human Genome Center, Institute of Medical Science, The University of Tokyo, Tokyo, Japan; Departments of ²Urology and ³Tumor Pathology, Kochi Medical School, Nankoku, Japan; ⁴Department of Urology, Kyoto Prefectural University of Medicine, Kyoto, Japan; and ⁵Department of Urology, Iwate Medical University, Morioka, Japan
Received 9/13/05; revised 1/11/06; accepted 2/22/06.

Grant support: Japan Society for the Promotion of Science Research for the Future Program grant #00L01402 (Y. Nakamura).

The costs of publication of this article were defrayed in part by the payment of page charges. This article must therefore be hereby marked *advertisement* in accordance with 18 U.S.C. Section 1734 solely to indicate this fact.

Requests for reprints: Hidewaki Nakagawa, Laboratory of Molecular Medicine, Human Genome Center, Institute of Medical Science, The University of Tokyo, 4-6-1 Shirokanedai, Minato-ku, Tokyo 108-8639, Japan. Phone: 81-3-5449-5375; Fax: 81-3-5449-5124; E-mail: hidewaki@ims.u-tokyo.ac.jp.

© 2006 American Association for Cancer Research.

doi:10.1158/1078-0432.CCR-05-1995

In this study, through intensive immunohistochemical staining, we show the relationship between MICAL2-PVs expression and clinicopathologic variables, including Gleason score and the expression status of c-Met. Our studies disclose the biological significance of MICAL2-PVs overexpression in progression of prostate cancer cells.

Materials and Methods

Cell lines. Human prostate cancer cell lines LNCaP, PC-3, DU145, and COS7 were obtained from the American Type Culture Collection (Rockville, MD). All of them were cultured as monolayers in appropriate medium supplemented with 10% fetal bovine serum. Cells were maintained at 37°C in an atmosphere of humidified air with 5% CO₂.

Selection of a candidate gene and Northern blot analysis. Using the gene expression profile analysis of 20 clinical prostate cancers (5), we selected several up-regulated genes whose expression ratio was >5.0 in >50% of informative cases, and we focused on one expressed sequence tag (EST) (accession no. AF052170). To confirm overexpression of a gene corresponding to this EST, we extracted total RNAs from prostate cancer cell lines using TRIzol reagent (Invitrogen, Carlsbad, CA) and did Northern blot analysis. After treatment with DNase I (Nippon Gene, Osaka, Japan), mRNA was purified with Micro-FastTrack (Invitrogen), according to the manufacturer's protocols. A 1-μg aliquot of each mRNA from prostate cancer cell lines and those isolated from normal human heart, liver, kidney, lung, bone marrow, pancreas, and prostate (BD Biosciences, Palo Alto, CA) were separated on 1% denaturing agarose gels and transferred onto nylon membranes. The 252-bp probes specific to AF052170 were prepared by PCR using the following primer set: forward, 5'-TGAAGCAACAAGAGAGGAGGAG-3' and reverse, 5'-CCGTGTGGCAGCTGTAATGATTA-3'. Hybridization with a random-primed, α³²P-dCTP-labeled probe was carried out according to the instructions for Megaprime DNA labeling system (Amersham Biosciences, Buckinghamshire, United Kingdom). Prehybridization, hybridization, and washing were done according to the supplier's recommendations. The blots were autoradiographed with intensifying screens at -80°C for 7 days. Human multiple-tissue Northern blots (BD Biosciences) were also hybridized with the ³²P-labeled AF052170-specific probe and analyzed.

Cloning the full length of MICAL-PVs. The further 3' portion of this cDNA clone, AF052170, was obtained by 3'-rapid amplification of cDNA ends (RACE) using a Marathon cDNA amplification kit (BD Biosciences). One microgram of mRNA from the human prostate cancer cell line LNCaP was reversely transcribed using Marathon cDNA synthesis primer and avian myeloblastosis virus reverse transcriptase (BD Biosciences). Marathon cDNA adaptors were added to the 5' and 3' end of the cDNA by T4 DNA ligase (BD Biosciences). The cDNA was amplified by PCR using the adaptor primer AP1 and the primer specific to AF052170, GSP1 (5'-CCITTAACCTGGGAGGCAGCGAC-3'). The product was amplified by nested PCR using the nested adaptor primer AP2 and the nested primer specific to AF052170, GSP2 (5'-CGTGTGTACGTGATGGAACGGCTGA-3'). The amplified cDNA fragments were directly sequenced using ABI 3700 DNA Analyzer (Applied Biosystems, Foster City, CA). The cDNA sequences were determined as described in the instructions of the kit. The 5' region of AF052170 was obtained by exon connection experiments using cDNA prepared from LNCaP as a template.

Preparation of polyclonal antibody to MICAL2-PVs. Plasmid clone designed to express His-tagged 137-amino-acid peptide (codon 827-963) corresponding to COOH-terminal of MICAL2-PVa was prepared using pET21 vector (Novagen, Madison, WI). This 137-amino-acid region is common in two variant transcripts and corresponds to its COOH-terminal region (codon 806-942) of MICAL2-PVb but is not present in MICAL2. The recombinant protein was expressed

in *Escherichia coli*, BL21 codon-plus strain (Stratagene, La Jolla, CA), and purified using Ni-resin according to the supplier's protocol (Qiagen, Inc., Valencia, CA). Proteins contaminated from *E. coli* were removed by anion exchange high-performance liquid chromatography. The purified protein was inoculated into two rabbits, and the immune sera were purified on affinity columns according to standard methodology.

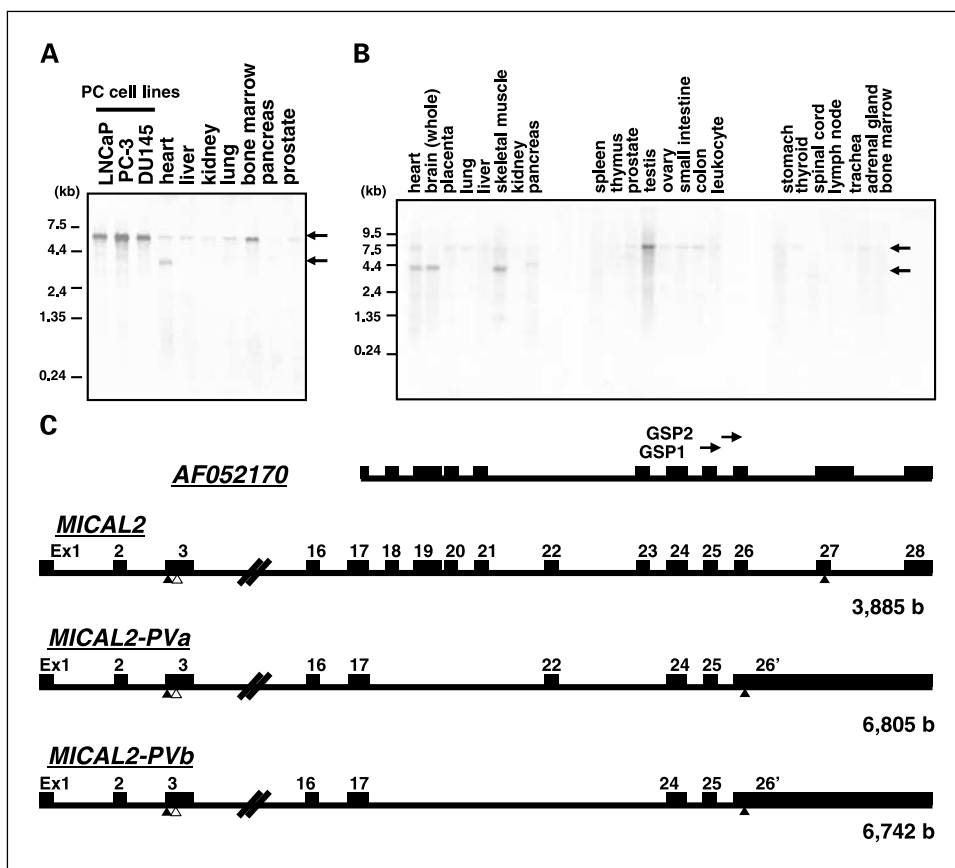
Immunoblot analysis. We examined endogenous expression of MICAL2-PV protein in prostate cancer cell lines LNCaP, DU145, and PC-3. COS7 cells that were transfected with pcDNA3.1-MICAL2-PVa-myc/His or pcDNA3.1-MICAL2-PVb-myc/His (for exogenous myc/His-tagged MICAL2-PV protein) were used as a positive control, and those transfected with pcDNA3.1 vector (mock) were used as a negative control of MICAL2-PV. Cell lysates were separated on 10% SDS-PAGE gels, transferred to nitrocellulose membranes (Amersham Biosciences), and incubated with a 1:500 diluted solution of anti-MICAL2-PV polyclonal antibody (pAb; 100 μg/mL) as a primary antibody. After incubation with sheep anti-rabbit IgG-horseradish peroxidase as a secondary antibody (Amersham Biosciences), signals were visualized with enhanced chemiluminescence kit (Amersham Biosciences).

Tissue samples and immunohistochemical study. Twenty-seven specimens of primary prostate cancer were obtained with the appropriate informed consent by radical prostatectomy at Department of Urology, Kochi Medical School and Kochi Prefectural Aki Hospital between 2001 and 2004. Representative section slides were obtained from the 27 specimens after fixation by formalin and being embedded in paraffin and then used for estimating the proportion of immunologic staining positive cells in the carcinoma, prostatic intraepithelial neoplasia, and normal tissues. To further investigate MICAL2-PV expression in a larger number of tumor specimens, tissue microarray samples containing 78 prostate cancer specimens (AccuMax Array, Petagen, Inc., Seoul, Korea), for which the mean age of the patients was 63.1 years (range, 43-79 years), were obtained also. Histopathologic classifications, including Gleason score, were done using the tumor-node-metastasis system (*Tumor-Node-Metastasis Classification of Malignant Tumors*, 6th edition, 2002). Immunohistochemical study was carried out using the Ventana automated immunohistochemical systems (Discovery, Ventana Medical systems, Inc., Tucson, AZ). Sections were incubated with a 1:20 diluted solution of purified anti-MICAL2-PV pAb (100 μg/mL) or a 1:50 diluted solution of anti-c-Met pAb (c-12, Santa Cruz Biotechnology, Inc., Santa Cruz, CA), for 16 minutes. The automated protocol is based on an indirect biotin-avidin system using a biotinylated universal secondary antibody and diaminobenzidine substrate with hematoxylin counterstaining. The specificity of the binding was confirmed by negative staining using rabbit nonimmune serum as primary antibody.

Scoring of immunohistochemical staining. To evaluate both the intensity of staining and the proportion of the positive-stained cells, we used a scoring method reported previously (11). Regarding the morphology and the intensity of MICAL2-PV or c-Met expression, positive staining of anti-MICAL2-PV or anti-c-Met antibody was defined as follows: score 1 for variable weak cytoplasmic staining, score 2 for segmental and apical granular cytoplasmic staining, and score 3 for diffuse continuous and intense cytoplasmic staining. For each score, the proportion of cells with the score was estimated visually. A combined weighed score (MICAL2-PV immunohistochemical score or c-Met immunohistochemical score) consisting of the sum of the proportion of cells with each score was calculated for each sample as described previously (11). For example, a case with 70% score 3 staining, 20% score 2 staining, and 10% score 1 staining would be scored as follows: 70 × 3 + 20 × 2 + 10 × 1 = 260. The maximum score should be 300.

Statistical analysis. The correlations between MICAL2-PV expression levels and clinicopathologic variables (age, preoperative serum prostate-specific antigen, tumor classification, lymph node metastasis, Gleason score, and lymphatic or vascular invasion) were evaluated using the Kruskal-Wallis and Mann-Whitney *U* tests. Association

Fig. 1. A, Northern blot analysis of a gene corresponding to expressed sequence tag AF052170 in prostate cancer cell lines (LNCaP, DU145, and PC-3) and normal human tissues (heart, liver, kidney, lung, bone marrow, pancreas, and prostate). About 7-kb transcript corresponding to the full-length *MICAL2-PV* was observed abundantly in three prostate cancer cell lines (LNCaP, PC-3, and DU145) and normal bone marrow compared with other normal adult tissues, including the prostate. On the other hand, about 4-kb transcript corresponding to the previously reported *MICAL2* was not expressed in prostate cancer cell lines. **B,** Northern blot analysis of a gene corresponding to expressed sequence tag AF052170 in normal adult human tissues. The 7-kb transcript corresponding to the full-length *MICAL2-PV* was observed abundantly in normal testis and prostate cancer cell lines, whereas the 4-kb transcript corresponding to the *MICAL2* was observed in heart, brain, and skeletal muscle. **C,** genomic structure of *MICAL2* and its novel variants *MICAL2-PVa* and *MICAL2-PVb*. Expressed sequence tag AF052170 was the probe for the microarray analysis. Full-length cDNA sequences of *MICAL2* (accession no. NM.014632), *MICAL2-PVa* (accession no. AB126828), and *MICAL2-PVb* (accession no. AB126829) were 3,885-, 6,805-, and 6,742-bp long, respectively. Exons are represented by black boxes. Black arrowheads indicate the stop codon and open arrowheads the first methionine.



between *MICAL2-PV* immunohistochemical scores and c-Met immunohistochemical scores was determined using the Spearman rank correlation coefficient test.

Small interfering RNA-expressing constructs and colony formation/MTT assay. We used small interfering RNA (siRNA) expression vector (psiU6BX3.0) for examining RNA interference effect to the target gene, *MICAL2-PV*, as described previously (12). The target sequences for *MICAL2-PV* are 5'-GCTGCTGGCCCTCCATATCA-3' (si#1) and 5'-TGCTFACAACTACTGCTAC-3' (si#2). The sequence of 5'-GAAGCAGCAGCAGCTTCTTC-3' (si#EGFP) corresponding to *EGFP* was used as a negative control. Human prostate cancer cell lines PC-3 and LNCaP were plated onto 10-cm dishes (5×10^5 per dish) and transfected with each of psiU6BX derivative clones that were designed to express siRNA

for the target sequence of *EGFP* or *MICAL2-PV* using FuGene6 reagent (Roche Diagnostics, Mannheim, Germany). Cells were selected in the culture medium containing 0.8 mg/mL Geneticin for 1 week and harvested 48 hours after transfection for reverse transcription-PCR analysis to validate knockdown effect on *MICAL2-PV*. The primers of reverse transcription-PCR were 5'-GCAGGATATCTTGAGAAA-3' and 5'-CCAGGATCTGCACAAATACA-3' for *MICAL2-PV* and 5'-TTGGCTTGACTCAGGATTTA-3' and 5'-TGGACTTGGGAGAGGACTGG-3' for β -actin, which was used to quantify the amount of cDNA input. After 7 days of incubation, these cells were fixed with 100% methanol and stained with Giemsa solution to evaluate the colony formation, and cell viability was evaluated by 3-(4,5-dimethylthiazol-2-yl)-2,5-diphenyltetrazolium bromide (MTT) assay. Cells (5×10^4) on six-well plates were transfected with siRNA-expressing vector or control vector using FuGene6 (Roche Diagnostics) according to the supplier's protocol. Cell-counting kit 8 (DOJINDO, Kumamoto, Japan) was added to each dish at a concentration of 1:10 volume, and the plates were incubated at 37°C for an additional 2 hours. Absorbance was then measured at 490 nm, and at 630 nm as reference, with a Microplate Reader 550 (Bio-Rad Laboratories, Hercules, CA).

Results

Identification and cloning of the full-length *MICAL2-PVs*. Through our earlier genome-wide expression analysis of prostate cancers using a cDNA microarray (5), we identified several genes commonly up-regulated in prostate cancer cells, and we here focused on one gene corresponding to an EST sequence (accession no. AF052170). Northern blot analysis revealed that a 7-kb transcript was commonly overexpressed in

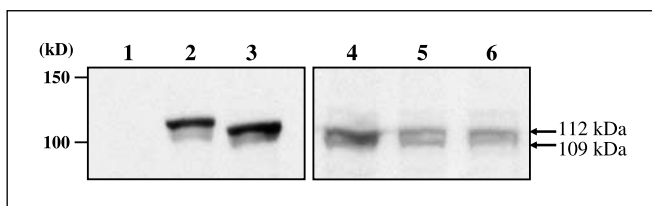


Fig. 2. Immunoblot analysis using purified polyclonal antibody specific to the novel variants *MICAL2-PVs*. Specificity of anti-*MICAL2-PV* pAb was indicated by detection of exogenous *MICAL2-PVs* in COS7 and endogenous *MICAL2-PVs* expression in three prostate cancer cell lines. Lane 1, COS7 cells transfected with mock pcDNA3.1; lane 2, COS7 cells transfected with pcDNA3.1/*MICAL2-PVa*; lane 3, COS7 cells transfected with pcDNA3.1/*MICAL2-PVb*; lane 4, LNCaP prostate cancer cell line cells; lane 5, DU145 prostate cancer cell line cells; lane 6, PC-3 prostate cancer cell line cells. The 112- and 109-kDa bands correspond to *MICAL2-PVa* and *MICAL2-PVb*, respectively.

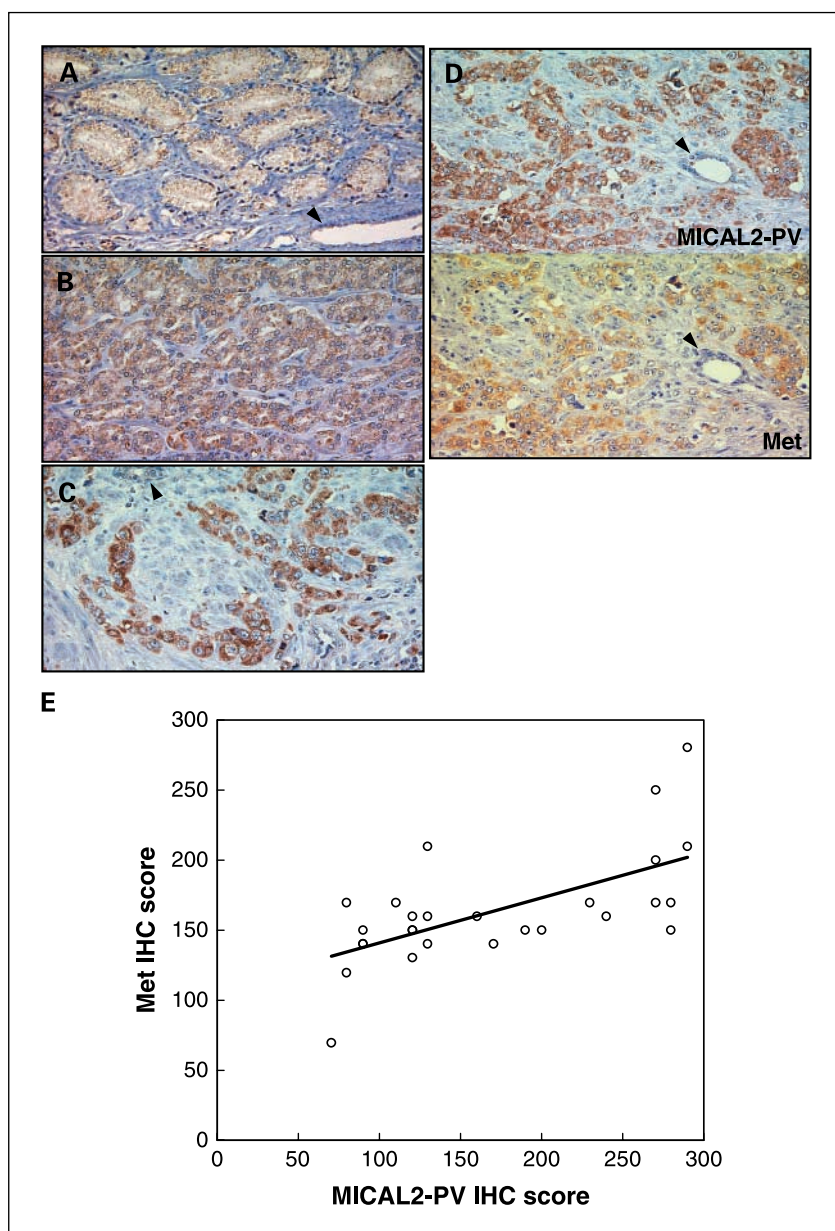


Fig. 3. Scoring evaluation in immunohistochemical staining with anti-MICAL2-PV antibody, indicating variable intensities of cytoplasmic staining. *A*, weak signal (score 1); *B*, segmental and apical granular pattern (score 2); *C*, diffuse continuous and intense pattern (score 3). *D*, two consecutive sections that were stained with anti-MICAL2-PV or anti-c-Met antibody. Double-positive immunoreactions were observed in most tumor cells. Adjacent normal prostatic epithelium revealed very weak expression of MICAL2-PV (*A*, *C*, and *D*; arrowheads). *E*, relationship between MICAL2-PV and c-Met IHC scores. Expression levels of MICAL2-PVs were significantly proportional to those of c-Met expression levels (Spearman rank correlation coefficient test, $\rho = 0.612$, $P = 0.0018$).

prostate cancer cells comparing with normal prostate (Fig. 1A), whereas a 4-kb transcript corresponding to the previously reported *MICAL2* cDNA (accession no. NM_014632) was not expressed in prostate cancer cell lines. Among the adult normal organs, this 7-kb transcript was most abundant in testis (Fig. 1B) and expressed in bone marrow (Fig. 1A), whereas the faint expression of this transcript was detectable in other organs, including vital organs. We attempted to isolate the full-length cDNA corresponding to the 7-kb transcript by exon connection experiments and 3'-RACE using cDNA prepared from prostate cancer cell line LNCaP. Then, we isolated two novel splicing variants of *MICAL2* that were different from the *MICAL2* transcript corresponding to NM_014632 reported previously. We named them *MICAL2-PVs* (prostate cancer variants), *MICAL2-PVa* and *MICAL2-PVb*, because they were overexpressed in prostate cancer. The *MICAL2* transcript is composed of 28 exons, whereas one of the *MICAL2* splicing variants,

MICAL2-PVa, has 21 exons with a large last exon (3885 bases), and the other variant, *MICAL2-PVb*, consisted of 20 exons as shown in Fig. 1C. Full-length cDNA sequences of *MICAL2-PVa* (accession no. AB126828) and *MICAL2-PVb* (accession no. AB126829) were 6,805-bp long and 6,742-bp long, respectively (Fig. 1C), encoding 976-amino-acid and 955-amino-acid proteins with a monooxygenase motif at its NH₂-terminal, a CasL domain, and a LIM domain that are conserved in members in the MICAL family.

Generating pAb specific to MICAL2-PV protein. To investigate the detail expression pattern of MICAL2-PV protein and characterize its biological functions, we generated pAb specific to MICAL2-PV, using the recombinant protein of the COOH-terminal region of MICAL2-PV, which was common in both MICAL2-PV variants but not contained in MICAL2, as an immunogen. We first did the immunoblot analysis to examine whether the purified anti-MICAL2-PV pAb (anti-MICAL2-PV

pAb) could recognize endogenous MICAL2-PV protein in prostate cancer cell lines, LNCaP, DU145, and PC-3 (Fig. 2). We used the exogenously introduced myc/His-tagged MICAL2-PVa and MICAL2-PVb proteins as positive controls. As shown in Fig. 2, this study validated that our anti-MICAL2-PV pAb could recognize both endogenous MICAL2-PVa and MICAL2-PVb (112 and 109 kDa, respectively) with high specificity and sensitivity.

Immunohistochemical study of prostatectomy specimens. We further did immunohistochemical staining of 27 clinical prostate cancer cases with anti-MICAL2-PV pAb. All 27 cases of prostate cancers expressed MICAL2-PV mainly in the cytoplasm, although staining patterns and intensities varied in individual cases (Fig. 3A-C). On the other hand, adjacent normal prostatic epithelium or prostatic intraepithelial neoplasia in the same patient revealed very weak or no signal for MICAL2-PV. Because each prostate cancer specimen apparently showed a different degree of staining intensity and different proportion of the staining-positive cell, we took these heterogeneity into consideration and applied the immunohis-

Table 1. Summary of the relationship between MICAL2-PV immunohistochemical scores and clinicopathologic factors in 105 patients with prostate cancers

	MICAL2-PV immunohistochemical score		P*
	n	Mean (SD)	
Age			
<60	31	172 (61)	0.5362
60-70	60	175 (62)	
>70	14	199 (74)	
Serum PSA [†] (ng/mL)			
<10	56	168 (64)	0.0865
10-20	20	185 (48)	
>20	16	195 (50)	
Tumor classification			
T _{2a} /T _{2b}	16	128 (33)	<0.0001
T _{2c}	25	157 (64)	
T _{3a}	38	179 (60)	
T _{3b}	22	221 (47)	
T ₄	4	245 (61)	
Lymph node metastasis			
Positive	4	260 (23)	0.0134
Negative	101	174 (63)	
Gleason score			
2-6	16	97 (18)	<0.0001
7	37	158 (43)	
8-10	52	216 (55)	
Lymphatic or vascular			
Positive	12	223 (55)	0.0058
Negative	93	171 (62)	

NOTE: Tumor classification was referred from Tumor-Node-Metastasis Classification (2002).

*Statistical significance was determined using Kruskal-Wallis and Mann-Whitney U tests.

† Data available in 92 cases.

Table 2. Relationship between MICAL2-PV immunohistochemical score and Gleason score in T₂ or T₃ staged PCs

Tumor classification	Gleason score	MICAL2-PV immunohistochemical score		P*
		n	Mean (SD)	
T ₂	2-6	13	97 (19)	<0.0001
	7	17	153 (30)	
	8-10	11	194 (68)	
T ₃	2-6	3	97 (9)	<0.0001
	7	20	163 (51)	
	8-10	37	219 (48)	

*Statistical significance was determined using Kruskal-Wallis test.

tochemical scoring system; a combined weighed score was given by the sum of the proportion (0-100%) of stained cells for which the score 1, 2, or 3 was given according to the signal intensity as described previously (11). MICAL2-PV immunohistochemical scores were calculated for 105 specimens on the tissue microarrays, based on this scoring criteria (see Materials and Methods); representative staining lesions scored as 1, 2, or 3 according to the intensity, and their morphologic evaluation are shown in Fig. 3.

To investigate the clinicopathologic significance of MICAL2-PV expression in prostate cancer tissues, we analyzed the relationship between the calculated immunohistochemical scores for MICAL2-PV and the clinicopathologic variables of 105 prostate cancer specimens, which is summarized in Table 1. Significant associations between MICAL2-PV immunohistochemical scores and several clinicopathologic factors ($P < 0.05$) were observed; in particular, it is notable that MICAL2-PV immunohistochemical scores were strongly correlated with tumor classification ($P < 0.0001$) and Gleason scores ($P < 0.0001$). We further divided these tumors into groups at the T₂ ($n = 41$) or T₃ ($n = 60$) stage by the size and confirmed that MICAL2-PV immunohistochemical score still revealed a strong correlation with Gleason score ($P < 0.0001$; Table 2), independent of the tumor size. Through immunohistochemical study, we noted that the cell staining pattern in each Gleason grade lesion was very homogeneous. Hence, we investigated the relationship between the Gleason grade and the MICAL2-PV intensity score and found that MICAL2-PV expression level was strongly correlated with Gleason grade ($P < 0.0001$; Table 3); higher Gleason-grade prostate cancers revealed higher expression levels of MICAL2-PV. There was no relationship between MICAL2-PV immunohistochemical score and preoperative serum PSA level ($P = 0.0865$; Table 1), which does not reflect the clinical behavior of prostate cancers (13).

MICAL2-PV expression was correlated with c-Met expression in prostate cancers. There are a number of accumulated evidences showing that scatter factor, hepatocyte growth factor, and its receptor c-Met are related to cancer progression, such as invasion or metastasis, and that c-Met expression was observed in high-grade prostate cancers and increased the incidence

Table 3. Relationship between MICAL2-PV expression level and Gleason grade in 53 lesions of prostate cancers

Gleason grade	MICAL2-PV expression level			P*
	Score 1	Score 2	Score 3	
2	5	0	0	<0.0001
3	14	6	0	
4	1	12	5	
5	0	2	8	

*Statistical significance was determined using χ^2 test.

of bone metastasis (14, 15). Similarly to the evaluation of MICAL2-PV expression, we also calculated c-Met immunohistochemical scores in 27 specimens from standard slides and examined the correlation between MICAL2-PV expression and c-Met expression (Fig. 3D). Interestingly, MICAL2-PV expression was positively correlated with c-Met expression ($\rho = 0.612$, $P = 0.0018$; Fig. 3E), suggesting a possible biological link between MICAL2-PV and c-Met expressions that affect prostate cancer progression (14, 15).

Knockdown of MICAL2-PV by siRNA suppressed prostate cancer cell viability. To investigate its potential of molecular therapeutic target for prostate cancers, we knocked down its endogenous expression in prostate cancer cell line PC-3 by mammalian vector-based RNA interference technology. The transfection of one of the siRNA-expressing vectors, si#2, clearly reduced the endogenous expression of MICAL2-PV (Fig. 4A). This knockdown effect by the siRNA on MICAL2-PV mRNA resulted in drastic growth suppression in colony formation assay as well as MTT assay (Fig. 4B and C). The similar results were obtained when we used another prostate cancer cell line LNCaP (data not shown). These findings

strongly suggest that overexpression of MICAL2-PV in prostate cancer cells is likely to be associated with prostate cancer cell viability and support its potential of molecular therapeutic target for prostate cancers.

Discussion

MICAL family was initially identified as a molecule interacting with CasL and vimentin, a major component of the intermediate filaments, implicating its role as a cytoskeletal regulator that connects CasL to intermediate filaments (6). Recently, Fischer et al. (16) reported a possible association of MICAL1 and MICAL3 with microtubule cytoskeleton in their immunofluorescence analysis. Although the results in these reports suggest a possible association between MICAL2-PV and cytoskeleton, we observed no change in the cell morphology or cytoskeletal structure of cells in which MICAL2-PV was overexpressed or knocked down (data not shown).

Drosophila MICAL interacts with plexin A and is required for semaphorin 1a/plexin A-mediated repulsive axon guidance. Vertebrate orthologues of *Drosophila* MICAL was also indicated to interact with plexins (7). Semaphorins are secreted and membrane-bound proteins that control axon guidance through their receptors, plexins (8, 17), and these molecules play essential roles in axon guidance and neuronal development. Invasive growth is a hallmark during the development of the nervous system (8), and these molecules mentioned above, including MICALs, are likely to function in promotion and invasion of cancer cells in the similar manner. Furthermore, a novel biological function of semaphorins and plexins was recently documented; plexin B1 (semaphorin 4D receptor) was shown to form a complex with c-Met, which shares structural homology with plexins in the extracellular domain. Binding of semaphorin 4D to plexin B1 was indicated to activate c-Met and then make tumor cells more invasive (9). Overexpression

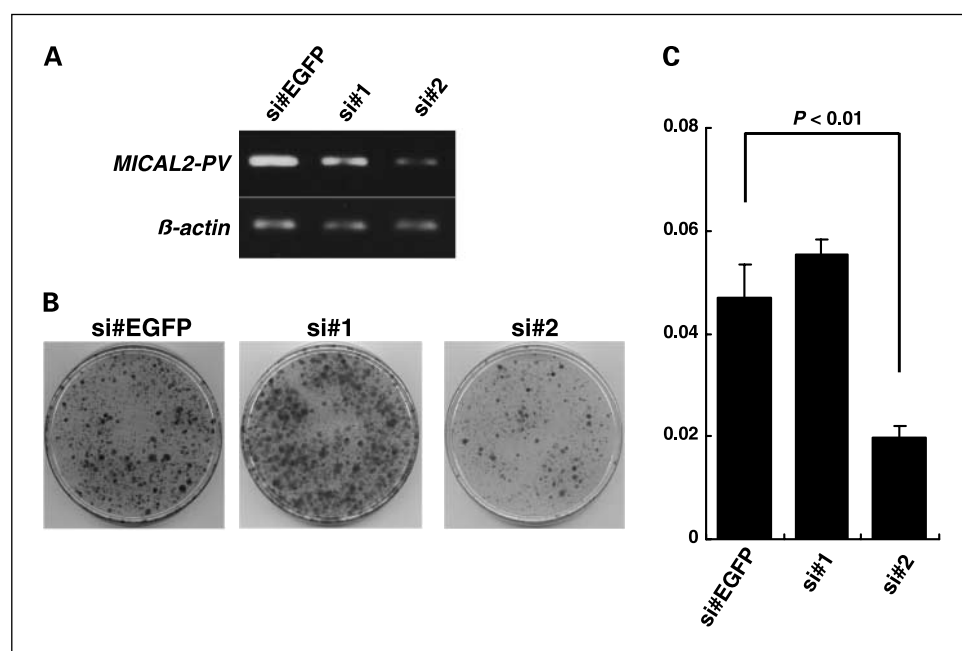


Fig. 4. Knockdown effect of MICAL2-PV-specific siRNA on prostate cancer cell line. Either of two siRNA expression vectors to MICAL2-PV (si#1 and si#2) or one siRNA expression vector to EGFP (si#EGFP) as a negative control was transfected into PC-3 cells. **A**, semiquantitative reverse transcription-PCR indicated the knockdown effect on endogenous MICAL2-PV expression in PC-3 cells by transfection of si#2 vector but not by si#1 or si#EGFP. β -Actin was used as a quantitative control. **B** and **C**, effect of siRNA on viability of prostate cancer cell line. Colony formation assay (**B**) showed decrease in the numbers of colonies in PC-3 cells transfected with si#2 vector that revealed significant knockdown effect on MICAL2-PV expression. MTT assay (**C**) also showed the significant suppression of prostate cancer cell viability following transfection of si#2 vector. Columns, mean; bars, SD. Statistical analysis was done by means of the Student's *t* test.

of c-Met was frequently observed in a wide spectrum of malignancies, including prostate cancers, and it plays a key role in cancer progression (8, 18, 19). Our immunohistochemical study evidently showed that MICAL2-PV expression status was strongly associated with progressive nature of the disease, such as tumor classification, lymph node metastasis, lymphatic or vascular invasion, and Gleason score (Tables 1-3), and our findings prompted us to investigate a possible association of MICAL2-PVs with c-Met in prostate cancer progression. Interestingly, the MICAL2-PV expression levels were also significantly concordant with the c-Met expression levels ($P = 0.0018$). Considering the relationship between c-Met expression and high-grade prostate cancers (14) or high incidence of bone metastasis in prostate cancers (15), our results of the coexpression of c-Met and MICAL2 suggest that MICAL2-PVs may be involved in cancer progression of prostate cancer as well as Gleason score, probably in association with the activation of the c-Met pathway. Gleason grading system is one of the established indicators for progression and prognosis of prostate cancers, and high Gleason score implies that cancer cells are more proliferative, lose cell-to-cell contact for scattered growth, and become more invasive (20). Our immunohistochemical data suggested that MICAL2-PV expression might associate with progression of prostate cancers

(Tables 1-3) in the similar manner with Gleason score, and that it should have therapeutic implications especially in patients having prostate cancers with high Gleason score. Indeed, our siRNA study, which knocked down MICAL2-PV expression in prostate cancer cells, supports its potential of molecular therapeutic target for prostate cancer treatment. Because MICAL2-PVs have the conserved monooxygenase domain at its NH₂-terminal, this enzymatic activity, if it has, could be a good therapeutic target to inhibit the MICAL2-PV function as well as MICAL1 (7). At present, the functional significance of MICAL2-PVs in prostate cancers remains unclear both in terms of cancer epidemiology and molecular pathology, and more detailed investigation into its function in prostate cancers, with or without the association to c-Met, is required. Because the most prevalent prostate cancer marker, PSA, is not related to the volume or grade of prostate cancers and does not reflect well the clinical behavior of prostate cancers (13), novel markers reflecting the pathologic and clinical outcome of prostate cancers are required. Our results have indicated that MICAL2-PVs should represent a promising novel molecular marker for prostate cancer progression as well as Gleason score, at least, and could be a promising candidate for development of novel treatment to prostate cancers with high Gleason score.

References

1. Gronberg H. Prostate cancer epidemiology. *Lancet* 2003;361:859–64.
2. Han M, Partin AW, Piantadosi S, Epstein JI, Walsh PC. Era specific biochemical recurrence-free survival following radical prostatectomy for clinically localized prostate cancer. *J Urol* 2001;166:416–9.
3. Roberts SG, Blute ML, Bergstralh EJ, Slezak JM, Zincke H. PSA doubling time as a predictor of clinical progression after biochemical failure following radical prostatectomy for prostate cancer. *Mayo Clin Proc* 2001;76:576–81.
4. Roberts WW, Bergstralh EJ, Blute ML, et al. Contemporary identification of patients at high risk of early prostate cancer recurrence after radical retropubic prostatectomy. *Urology* 2001;57:1033–7.
5. Ashida S, Nakagawa H, Katagiri T, et al. Molecular features of the transition from prostatic intraepithelial neoplasia (PIN) to prostate cancer: genome-wide gene-expression profiles of prostate cancers and PINs. *Cancer Res* 2004;64:5963–72.
6. Suzuki T, Nakamoto T, Ogawa S, et al. MICAL, a novel CasL interacting molecule, associates with vimentin. *J Biol Chem* 2002;277:14933–41.
7. Terman JR, Mao T, Pasterkamp RJ, Yu HH, Kolodkin AL. MICALs, a family of conserved flavoprotein oxidoreductases, function in plexin-mediated axonal repulsion. *Cell* 2002;109:887–900.
8. Trusolino L, Comoglio PM. Scatter-factor and semaphorin receptors: cell signalling for invasive growth. *Nat Rev Cancer* 2002;2:289–300.
9. Giordano S, Corso S, Conrotto P, et al. The semaphorin 4D receptor controls invasive growth by coupling with Met. *Nat Cell Biol* 2002;4:720–4.
10. Conrotto P, Corso S, Gamberini S, Comoglio PM, Giordano S. Interplay between scatter factor receptors and B plexins controls invasive growth. *Oncogene* 2004;23:5131–7.
11. Luo J, Zha S, Gage WR, et al. Alpha-methylacyl-CoA racemase: a new molecular marker for prostate cancer. *Cancer Res* 2002;62:2220–6.
12. Anazawa Y, Nakagawa H, Furihata M, et al. PCOTH, a novel gene over-expressed in prostate cancers, promotes prostate cancer cell growth through phosphorylation of oncoprotein TAF-I β /SET. *Cancer Res* 2003;65:4578–86.
13. Stamey TA, Caldwell M, McNeal JE, Nolley R, Hemenez M, Downs J. The prostate specific antigen era in the United States is over for prostate cancer: what happened in the last 20 years? *J Urol* 2004;172:1297–301.
14. Pisters LL, Troncoso P, Zhou HE, Li W, von Eschenbach AC, Chung LW. c-Met proto-oncogene expression in benign and malignant human prostate tissues. *J Urol* 1995;154:293–8.
15. Knudsen BS, Gmyrek GA, Inra J, et al. High expression of the Met receptor in prostate cancer metastasis to bone. *Urology* 2002;60:1113–7.
16. Fischer J, Weide T, Barnekow A. The MICAL proteins and rab1: a possible link to the cytoskeleton? *Biochem Biophys Res Commun* 2005;328:415–23.
17. Winberg ML, Noordermeer JN, Tamagnone L, et al. Plexin A is a neuronal semaphorin receptor that controls axon guidance. *Cell* 1998;95:903–16.
18. Knudsen BS, Edlund M. Prostate cancer and the Met hepatocyte growth factor receptor. *Adv Cancer Res* 2004;91:31–67.
19. Kim SJ, Johnson M, Koterba K, Herynk MH, Uehara H, Gallick GE. Reduced c-Met expression by an adenovirus expressing a c-Met ribozyme inhibits tumorigenic growth and lymph node metastases of PC3–4 prostate tumor cells in an orthotopic nude mouse model. *Clin Cancer Res* 2003;9:5161–70.
20. Humphrey PA. Gleason grading and prognostic factors in carcinoma of the prostate. *Mod Pathol* 2004;17:292–306.